THE JOURNAL OF PHYSICAL CHEMISTRY Letters

Letter

pubs.acs.org/JPCL

Ultrafast Surface-Enhanced Raman Probing of the Role of Hot Electrons in Plasmon-Driven Chemistry

Nathaniel C. Brandt, Emily L. Keller, and Renee R. Frontiera*

Department of Chemistry, University of Minnesota, Minneapolis, Minnesota 55455, United States

Supporting Information

ABSTRACT: Hot electrons generated through plasmonic excitations in metal nanostructures show great promise for efficiently driving chemical reactions with light. However, the lifetime, yield, and mechanism of action of plasmon-generated hot electrons involved in a given photocatalytic process are not well understood. Here, we develop ultrafast surface-enhanced Raman scattering (SERS) as a direct probe of plasmon−molecule interactions in the plasmon-catalyzed dimerization of 4-nitrobenzenethiol to *p*,*p*′-dimercaptoazobenzene. Ultrafast SERS probing of these molecular reporters in plasmonic hot spots reveals transient Fano resonances, which we attribute to near-field coupling of Stokes-shifted photons to hot electron-driven metal photoluminescence. Surprisingly, we find that hot spots that yield more photoluminescence are much more likely to drive the reaction, which indirectly proves that plasmon-generated hot electrons induce the photochemistry. These ultrafast SERS results provide insight into the relative reactivity of different plasmonic hot spot environments and quantify the ultrafast lifetime of hot electrons involved in plasmon-driven chemistry.

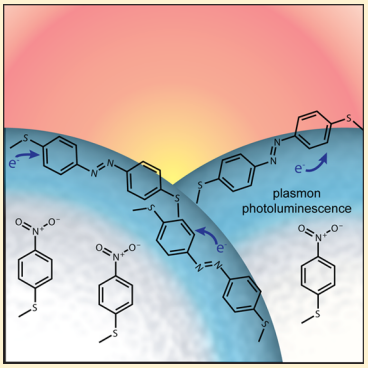

The efficient coupling of light to metallic nanostructures through localized surface plasmon resonances (LSPR) leads to numerous impactful applications, including light-driven phase changes and chemical reactions.[1−3] Plasmon-driven chemical or physical transformations typically arise either from plasmon-generated hot carriers or plasmon-driven localized heating, both of which preferentially occur in plasmonic hot spots.[2] In particular, many plasmon-driven chemical reactions are believed to occur as a result of plasmon-induced electronic excitations in adsorbed molecules, through either direct plasmon-driven excitation of a resonant molecular transition or indirect transfer of plasmon-generated hot electrons to accessible adsorbate orbitals.[2,4,5] In a notable example, indirect transfer of plasmon-generated hot electrons to adsorbed H_2 molecules has been experimentally shown to result in H−H bond scission.[4,5] However, the impact of the lifetime, yield, and energetic distribution of these plasmon-derived hot electrons on driving photochemical reactions is currently unknown. Additionally, the dependence of these properties on the nature of the plasmonic surface is unclear. As plasmonic dynamics inherently occur on femtosecond to picosecond time scales,[6,7] further mechanistic knowledge of plasmon-driven chemical reactions necessitates real time probing of the ultrafast molecular response to plasmon excitation. An ultrafast molecular understanding of plasmon-driven chemical reactions will be important in the optimization and practical use of such processes.

Previous investigations of the ultrafast response of plasmonic metallic nanostructures have largely examined the response of the nanostructure itself, and measurements of the proximal molecular response have been limited. From this work, a consensus view of the ultrafast photophysical response of plasmonic nanostructures has emerged.[2,6−8] When the LSPR of the nanostructure is excited by light, the coherent electronic motion that is induced by the external field is quickly damped to form electron−hole pairs within approximately 10 fs. These electron−hole pairs subsequently thermalize through electron−electron scattering over 10−100 fs to yield an incoherent Fermi−Dirac distribution of hot electrons and holes.[1,2,7,9,10] In the direct mechanism for plasmon-driven photochemistry, the transfer of the electrons occurs at the metal−molecule interface via resonant plasmon-driven electron excitation, while in the indirect mechanism, hot carriers are transferred from the thermalized Fermi−Dirac distribution on the nanostructure to adsorbate orbitals.[2,11] This process is in competition with other hot electron loss mechanisms, principally electron−phonon scattering, which occurs over approximately 1−10 ps,[9] followed by equilibration of the hot nanostructure lattice with the surroundings over the course of 100 ps−1 ns.[6] Alternatively, electrons and holes may also radiatively recombine to yield plasmon-driven metal photoluminescence. Measurements of plasmonic photoluminescence typically have determined lifetimes for these hot electrons of several picoseconds.[12,13] In this Letter, we use photoluminescence as a generic term for any process in which light is emitted or scattered from a photoexcited sample, inclusive of coherent processes such as electronic Raman scattering.

Importantly, this description lacks a real time view of hot electron generation and transfer from the point of view of a

Received: June 30, 2016
Accepted: August 1, 2016
Published: August 4, 2016

DOI: 10.1021/acs.jpclett.6b01453
J. Phys. Chem. Lett. 2016, 7, 3179−3185

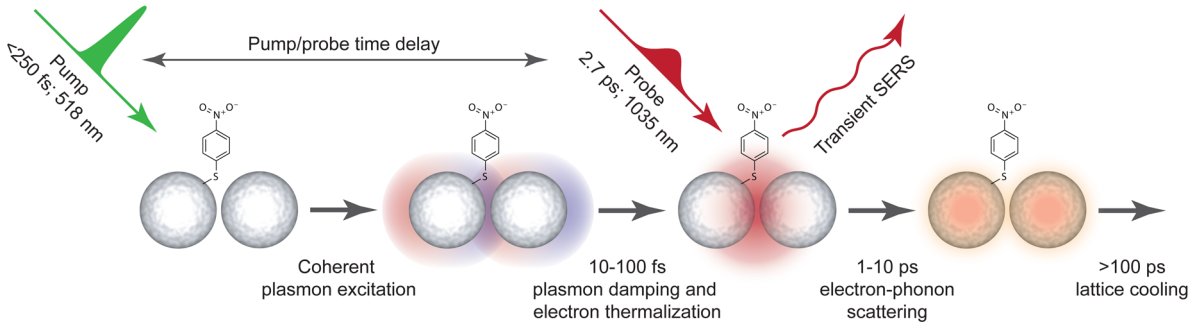

Figure 1. Schematic representation of ultrafast plasmon excitation and plasmon-driven molecular dynamics measurement scheme. Plasmons are excited by a 518 nm pump pulse, launching short-lived coherent oscillations. These thermalize over 10−100 fs, yielding a hot electron distribution, from which hot electrons may be transferred to adsorbed molecular reporter molecules. Transient plasmon-driven molecular dynamics are obtained through ultrafast SERS using a probe pulse during the 1−10 ps hot electron lifetime.

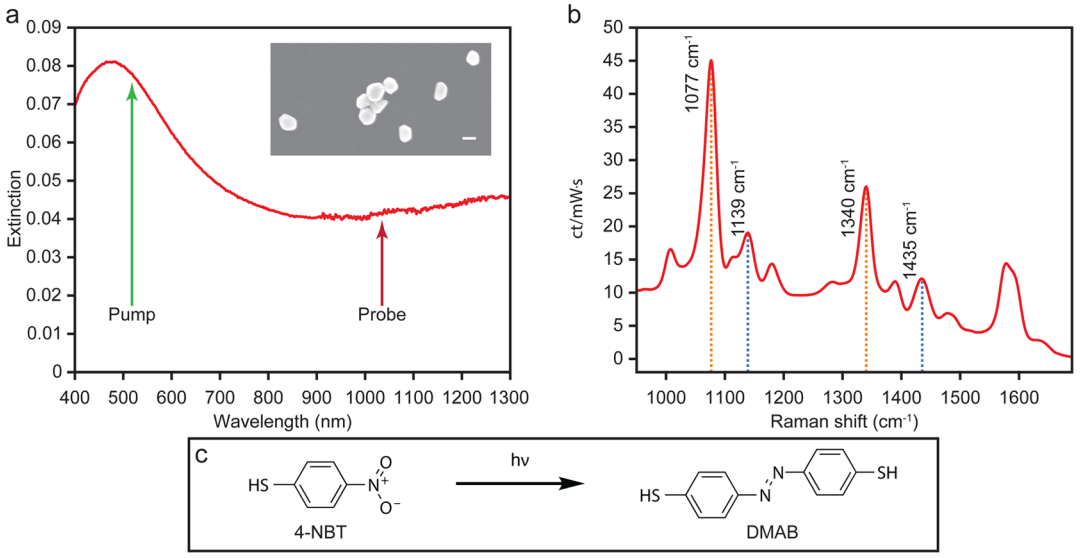

Figure 2. (a) Representative extinction spectrum of aggregated colloidal AgNPs used as the plasmonic substrate in all measurements, with pump and probe pulse wavelengths noted. The inset shows an SEM image of the AgNPs. The scale bar is 100 nm in length. (b) SER spectrum of substrates, with prominent 4-NBT (1077 and 1340 cm^{-1}) and DMAB (1139 and 1435 cm^{-1}) peaks identified. (c) Plasmon-driven photochemical conversion of 4-NBT to DMAB.

molecular adsorbate. A real time investigation of plasmon-driven chemistry through hot electron transfer from a molecular perspective may be obtained from a measurement that exhibits both ultrafast time resolution as well as molecular specificity. In this work, we introduce a pump/probe technique based on ultrafast surface-enhanced Raman scattering (SERS)[14,15] as a molecule-specific probe of the ultrafast responses of molecules adsorbed to plasmonic nanostructures during the picosecond time scale over which hot electron transfer occurs. We used ultrafast SERS to examine the plasmon-driven photophysical dynamics of a model system consisting of 4-nitrobenzenethiol (4-NBT) adsorbed to aggregated colloidal silver nanoparticles (AgNPs). Because 4-NBT readily undergoes plasmon-driven dimerization to *p,p′*-dimercaptoazobenzene (DMAB),[16−19] the photophysical responses that we obtained also yielded direct evidence of the role of hot electrons in the plasmon-driven dimerization reaction.

Our ultrafast SERS method for extracting plasmon-driven molecular responses is summarized relative to the time scales of electron and phonon interactions following LSPR excitation in Figure 1. The instrument is described in detail in the Supporting Information and Figure S1. Plasmonic responses are first excited using a femtosecond pump pulse. The vibrational signature of adsorbed reporter molecules is then probed via spontaneous SERS using a time-delayed picosecond probe pulse. Because SERS is primarily plasmon-driven,[20] SER spectra are inherently sensitive only to molecules adsorbed in plasmonic hot spots,[21] thereby limiting ultrafast responses only to molecules that are located in the most highly enhancing regions. Thus, ultrafast SERS offers a direct observation of the coupled molecular-plasmonic system in real time.

The plasmonic substrate used in our measurements was a solution of AgNPs (Figure 2a inset; measured diameter 120 ± 20 nm) aggregated through electrostatic interactions into inhomogeneous clusters. These plasmonic substrates are frequently used for single-molecule SERS measurements due to the facile creation of hot spots with strong field enhancements.[22,23] Aggregation yields hot spots in the junctions between nanoparticles through LSPR coupling, in which field enhancement is much greater than would be encountered on the surface of a single nanoparticle.[20,24,25] Additionally, LSPR coupling results in a broad LSPR extinction band that allows for efficient plasmon excitation and efficient

DOI: 10.1021/acs.jpclett.6b01453
J. Phys. Chem. Lett. 2016, 7, 3179−3185

SERS probing using widely separated pump and probe wavelengths (Figure 2a).

In this work, we utilized a high-repetition-rate laser (Clark-MXR Impulse) producing <250 fs, 1035 nm pulses, with nJ energies at a 24.5 MHz repetition rate, which allowed for high signal-to-noise ratio SER spectra while incurring minimal sample damage. We photoexcited the sample using a 518 nm femtosecond pulse and probed with a 2.7 ps narrow-band pulse at 1035 nm. We performed ultrafast SERS measurements in a transmissive geometry and detected the Stokes-shifted scattering on an InGaAs array (Princeton Instruments PyLoN-IR 1.7).

A representative SER spectrum of 4-NBT adsorbed to the aggregated AgNP substrate is displayed in Figure 2b, which shows prominent vibrations arising from 4-NBT as well as DMAB. For the purposes of this work, we limit our major analyses to the four largest peaks, located at 1077 and 1340 cm^{-1}, which correspond to 4-NBT, and at 1139 and 1435 cm^{-1}, which correspond to DMAB.[26,27] The significant population of DMAB is the result of the well-known plasmon-driven chemical dimerization of 4-NBT to DMAB (Figure 2c), which has been previously observed and characterized on a variety of plasmonic substrates.[16−18] We attribute the appearance of DMAB in the unperturbed sample to exposure to ambient light sources prior to data collection. During the course of our measurements, the sample was essentially static. This indicated that the vast majority of hot spots that were capable of dimerizing 4-NBT to DMAB had already done so prior to our measurements.

Ultrafast SERS measurements were collected at various pump/probe time delays and processed by subtracting SER spectra taken with the pump pulse blocked from identical spectra collected with the pump pulse present. An additional subtraction step, to remove the static effects of pump pulse propagation through the highly scattering AgNP suspension, is described in detail in the Supporting Information. Ultrafast SER difference spectra taken at time delays ranging from −20 to 50 ps are shown in Figure 3a. Transient dispersive line shapes are observable at all prominent 4-NBT and DMAB vibrations, which persist in intensity for approximately 10 ps after plasmon excitation. Within the spectral resolution of our instrument, we do not see frequency shifts indicative of molecular heating, which have previously been carefully quantitated for 4-NBT on gold surfaces.[28] These dispersive features were fit to a Fano line shape as other fit functions resulted in poor fitting, particularly for the positively sloped regions at around 1050 and 1300 cm^{-1}. Fit functions and additional fit parameters are included in the Supporting Information. Fitting of the extracted amplitude of the 1139 cm^{-1} feature yields a lifetime of 3.9 ± 0.1 ps (Figure 3b; see Figure S2 for amplitude extraction). Fits to the other prominent features yield similar lifetimes (Figure S3). Notably, this timescale matches literature values for plasmon-generated hot electron lifetimes,[6,7] and thus, it is clear that the transient response is the result of a hot electron-driven perturbation. To identify the mechanism of this perturbation, we turn to analysis of the line shapes.

The appearance of dispersive line shapes is not entirely unexpected as previous ultrafast surface-enhanced stimulated Raman[29,30] and steady-state spontaneous Raman[31] measurements have reported the appearance of Fano line shapes arising from interference between narrow Raman-active molecular transitions and a broad electronic resonance of the SERS substrate. However, our current results differ from these previous reports in several important ways. First, the Fano line

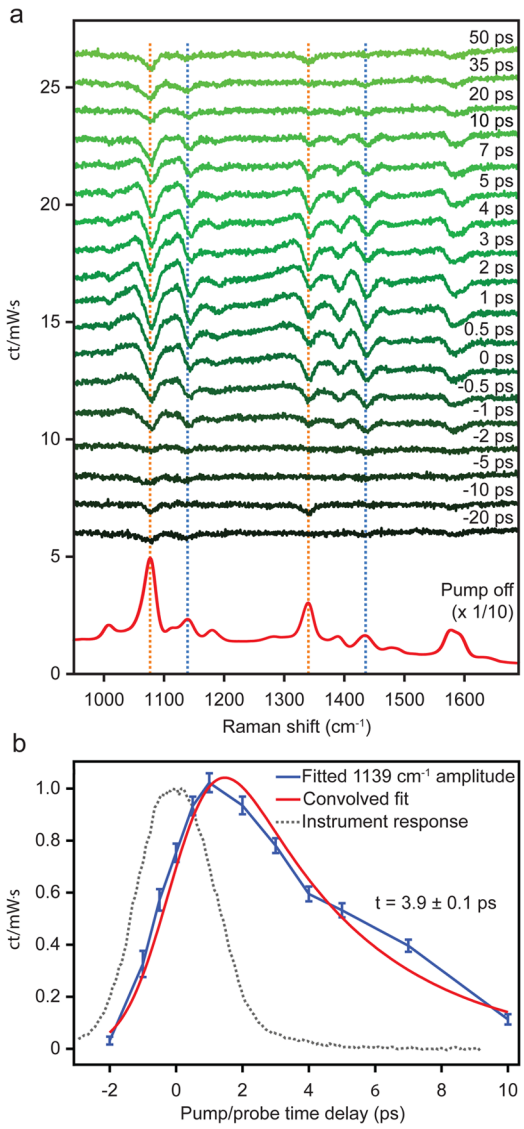

Figure 3. (a) Ultrafast SER difference spectra (obtained as described in the Supporting Information) taken at pump/probe time delays ranging from −20 to +50 ps, showing transient Fano features at prominent 4-NBT and DMAB Raman peaks. (b) Fitted amplitude of the 1139 cm^{-1} transient feature shown in (a).

shapes seen in surface-enhanced femtosecond stimulated Raman spectroscopy (FSRS) measurements result from a coherent Raman scattering process, whereas our measurements report transient dispersive spontaneous Raman line shapes. Additionally, the stimulated Raman measurements showed Fano line shapes only when both ultrafast pulses used in the FSRS measurement were present at the sample, while we observe long-lived dispersive line shapes that persist for several picoseconds after the pump pulse has left the sample. More recently, Fano line shapes have been reported in spontaneous SERS measurements;[31] however, in addition to appearing in the steady state, the reported line shapes were also far more broad than what we observe.

In these measurements, the appearance of Fano line shapes is evidence that the ultrafast SERS features are not solely arising as a result of transient LSPR shifts. In plasmonic nanoparticles, ultrafast transient absorption measurements have proven that photoexcitation results in a shift of the plasmon resonance due

DOI: 10.1021/acs.jpclett.6b01453
J. Phys. Chem. Lett. 2016, 7, 3179−3185

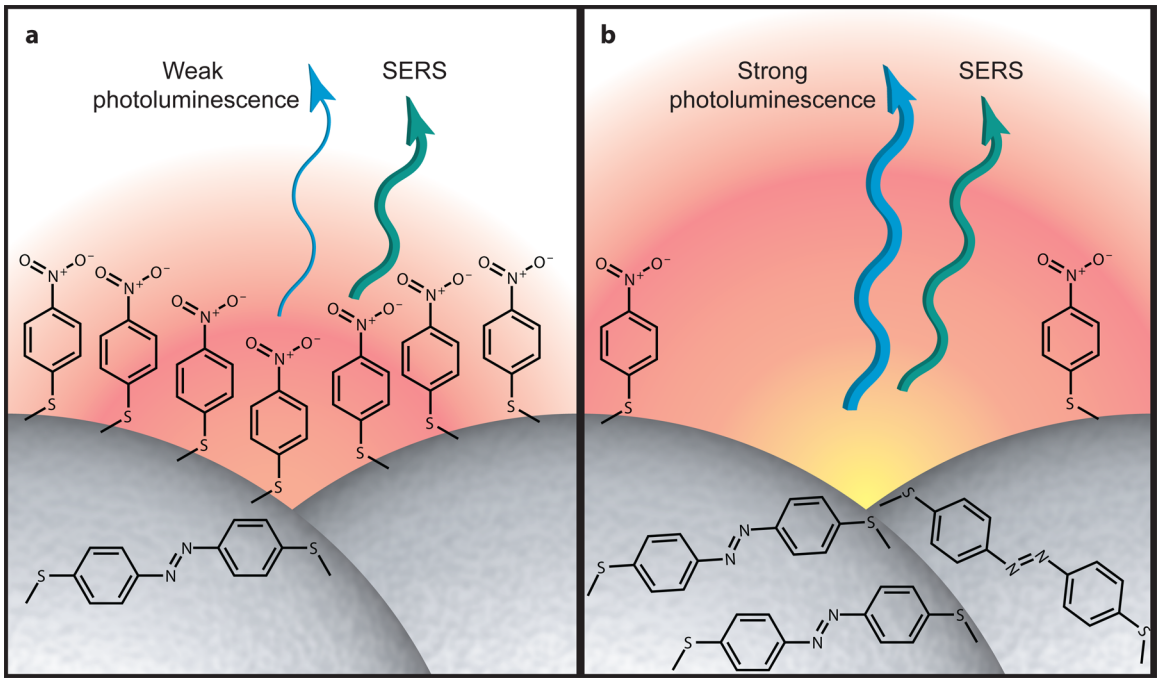

Figure 4. Schematic representation of low reactivity and high reactivity hot spots. (a) Low reactivity hot spot, showing SERS emission, relatively small population of DMAB relative to 4-NBT due to weak photoreactivity, and weak (or nonexistent) photoluminescence intensity, resulting in negligible transient Fano signal. (b) High reactivity hot spot, with similar SERS emission intensity but increased DMAB population (due to higher photoreactivity) and increased photoluminescence intensity relative to (a), which results in detectable transient Fano signal.

to the creation of a nonequilibrium electron distribution. Typically, when the slope of the LSPR is positive, there is a transient bleach, indicative of a red shift of the LSPR.[32] Shifts in the plasmon resonance would lead to an increase or decrease of the ultrafast SERS signal magnitude due to differences in the efficiency of coupling light into the nanostructure. This would result in either positive or negative Gaussian SERS features in the transient difference spectra but would not result in Fano line shapes.

We assign the Fano line shapes observed in our ultrafast SERS measurements to interference of each molecular vibration with plasmon-driven photoluminescence of the AgNPs. Here we use photoluminescence as a generic term for any optically initiated light generation from the sample, inclusive of processes such as electronic Raman scattering. Metal photoluminescence, which is greatly enhanced in plasmonic nanostructures, arises from radiative recombination of plasmon-driven electronic excitations, which may be either inter- or intraband in nature. Because our pump frequency falls well below the ∼4 eV photon energy necessary for interband excitation in Ag,[33] interband excitation is likely not significant in these samples. In general, intraband metal photoluminescence is characterized by a broad bandwidth consisting of both upconverted and downconverted emission, thus providing precisely the necessary frequency range to cause the interference that we observe.[13,34] The spectra in Figure 3a are offset but not baseline corrected; therefore, any directly observed transient photoluminescence in our ultrafast SERS measurements is contained within the baseline. In this case, the photoluminescence appears to be too weak to conclusively identify, and we conclude that we are heterodyne-detecting the photoluminescence through the stronger SERS signal.

The lifetime of the Fano response allows it to be explicitly assigned to AgNP photoluminescence. Plasmon-driven photoluminescence arises directly from plasmon-generated hot electrons, and thus, photoluminescence lifetimes are an excellent measurement of hot electron lifetimes.[12] Previously reported plasmon-generated photoluminescence lifetimes reflect this, with literature values ranging from 1.6 to 3.2 ps, which is in excellent agreement with our measured value of 3.9 ± 0.1 ps for the lifetime of the transient Fano feature at 1139 cm^{-1}.[12,13] Additionally, the amplitude of the transient Fano features shows a linear dependence on pump irradiance (Discussion in the Supporting Information and Figure S4), which is consistent with photoluminescence.[13,34] The nature of the ultrafast SERS measurement does not enable us to assign the origin of photoluminescence more specifically, but due to the coherent nature of the Fano interference process, it likely results from an electronic Raman process from the nonequilibrated hot electrons in the nanoparticles.[31,35,36] We turn now to interpretation of the nature of the coupling between the AgNP photoluminescence and SERS and its broader implications through analysis of the amplitudes of the transient Fano features.

Contained within the amplitudes of the transient Fano features is direct evidence of (i) a near-field coupling mechanism and (ii) the role of plasmon-generated hot electrons in the dimerization of 4-NBT to DMAB. All measurements were made on samples in which the reaction had already gone to completion; therefore, both the ground-state and transient SER spectra contain signatures from reactant and product species. The concentration of both reactants and products does not change during the ultrafast measurement. To extract this amplitude information, we begin with examination of the ground-state SER spectrum of our sample (Figure 2b). In this spectrum, the amplitudes of the peaks corresponding to 4-NBT are much larger than those corresponding to DMAB. When comparing the 1077 and 1340 cm^{-1} 4-NBT peaks to the

DOI: 10.1021/acs.jpclett.6b01453
J. Phys. Chem. Lett. 2016, 7, 3179−3185

1139 and 1435 cm^{-1} DMAB peaks, the amplitudes yield ratios of approximately 5:1 and 3:1, respectively. If we examine the ultrafast SER spectra (Figure 3a), however, the amplitudes of the *transient features* corresponding to peaks from either molecular species are instead very similar in amplitude, giving a ratio of 4-NBT/DMAB of approximately 1:1 when comparing the same sets of peaks. Surprisingly, the transient SERS features are much larger for product molecules as compared to those for reactant molecules.

This change in the ratio of 4-NBT/DMAB peak amplitudes in the transient versus ground-state spectra immediately implies that the coupling of plasmonic photoluminescence and Stokes-shifted SERS photons occurs in the near-field. If the coupling occurred in the far-field, then we would expect that the average hot spot to which any photoluminescence-emitting hot spot may couple would reflect the full distribution of hot spots in the sample. In this regime, we would then expect to observe an identical ratio of 4-NBT and DMAB amplitudes in the transient Fano features and the ground-state SER spectra. Because our observations do not support this scenario, our data therefore prove that the coupling is near-field in nature. Near-field localized coupling between Raman scattering and plasmonic nanostructures has been seen previously in super-resolution SERS but has not been previously observed for picosecond-scale phenomena such as plasmon-induced photoluminescence.[37]

The transient and ground-state 4-NBT/DMAB peak amplitude difference provides direct evidence of the role of hot electron involvement in the plasmon-driven dimerization of 4-NBT to DMAB. The amplitude ratio change from ground-state to transient SERS measurements proves that the presence of DMAB is correlated with the generation of sufficient photoluminescence to give detectable transient Fano responses. Additionally, the near-field nature of the coupling indicates that these two parameters are correlated on the single hot spot level. For clarity, we label the limiting cases as "low reactivity" and "high reactivity" hot spots, which are illustrated schematically in Figure 4. In the case of low reactivity hot spots (Figure 4a), the ratio of 4-NBT to DMAB is high as very little 4-NBT has reacted, and the plasmon-driven photoluminescence yield is low. In contrast, a high reactivity hot spot (Figure 4b) contains increased DMAB population relative to 4-NBT as well as increased photoluminescence yield and is more likely to yield a detectable Fano response. Because the AgNP photoluminescence is the direct result of plasmon-generated hot electrons, the correlation between photoluminescence and DMAB in the high reactivity hot spots signifies colocalization of plasmon-generated hot electrons and the presence of DMAB. Therefore, the 4-NBT/DMAB amplitude ratio difference in the transient Fano response indirectly proves that plasmon-generated hot electrons are responsible for the plasmon-assisted photochemical dimerization of 4-NBT to DMAB.

The correlation between the hot electron population and 4-NBT-to-DMAB conversion has significant mechanistic implications. An exclusively direct mechanism of plasmon-driven chemistry would preclude the existence of a significant population of hot electrons on the surface of the AgNP substrate.[2] In our measurements, however, the presence of photoluminescence is direct evidence that such a population exists. While this is not definitive proof of an exclusively indirect mechanism, it is nevertheless highly suggestive of a significant indirect component in the hot electron transfer mechanism.

We have demonstrated that ultrafast spontaneous SERS can be used to selectively probe ultrafast plasmon-driven dynamics in molecules adsorbed in plasmonic hot spots. Ultrafast SERS results obtained on aggregated AgNP substrates revealed transient dispersive line shapes appearing at Raman vibrations corresponding to both the 4-NBT molecular reporter as well as the DMAB photoproduct, which were identified as Fano line shapes arising from interference between the SERS photons and transient plasmon-driven AgNP photoluminescence or electronic Raman scattering. Through analysis of the change in the 4-NBT/DMAB amplitude ratio between the ground-state SER spectrum and the transient Fano line shapes, we conclude that the transient responses interrogate a specific subset of AgNP hot spots. Significantly, the increased presence of DMAB in the hot spots that produced the transient response is evidence that the plasmon-driven photochemical dimerization of 4-NBT to DMAB is the result of plasmon-generated hot electrons and suggests the significant role of an indirect charge-transfer mechanism. Because we have demonstrated that ultrafast SERS probing is capable of observing the role of hot electrons in a plasmon-driven photocatalytic process, we anticipate that ultrafast SERS probing of plasmon-driven molecular dynamics will be of great utility in future mechanistic studies of socially impactful plasmon-driven chemical and physical transformations.

EXPERIMENTAL METHODS

Sample Preparation. SERS samples were prepared using a 230 μL aliquot of an as-synthesized solution of AgNPs, following the Lee and Meisel synthesis,[38] to which we added 70 μL of a saturated 4-NBT aqueous solution (concentration measured by UV−visible spectroscopy to be approximately 150−200 μM). After approximately 10 min, AgNP aggregation was induced by adding 100 μL of a 0.1 M NaCl aqueous solution. Samples were stirred throughout the course of the experiment to refresh the sample in the spot size and to minimize precipitation of the aggregated particles. More detail is available in the Supporting Information, Methods.

Ultrafast SERS Measurements. Ultrafast SERS measurements were performed using a Yb-doped fiber-based amplified laser, which produced <250 fs pulses centered at 1035 nm at a 24.5 MHz repetition rate, with an average power of 20.5 W. To generate the picosecond probe pulse, 6 W of the incident beam entered a spectral filter constructed in a retroreflecting geometry.[39] The power of the probe beam at the sample was 16.8 mW, corresponding to a flux of 1.7×10^{21} photons/cm^2 s. The spectral width of the filtered output was 13.4 cm^{-1}, measured from the 801 cm^{-1} peak of cyclohexane. For the pump beam, 3 W of the fundamental laser output was focused onto a 3 mm BBO crystal to obtain a 518 nm, <250 fs pulse, which was delayed in time using a mechanical stage relative to the probe pulse. The power of the photoexcitation beam at the sample was 25 mW, corresponding to a flux of 1.3×10^{21} photons/cm^2 s. A 100 mm focal length achromatic lens focused the probe and pump beams onto the sample. Raman signals were detected using a 0.3 m spectrograph equipped with a 600 gr/mm, 750 nm blaze grating and a 1024 pixel liquid-nitrogen-cooled InGaAs photodiode array. The ultrafast SERS instrumentation that we used is described in more detail in the Supporting Information, Methods and Figure S1.

Data Collection and Analysis. Each ultrafast SER spectrum was obtained from five averaged frames that were integrated for 10 s each. For pump/probe measurements, pump/probe time delays

DOI: 10.1021/acs.jpclett.6b01453
J. Phys. Chem. Lett. 2016, 7, 3179−3185

were accessed in a randomized order. The spectra were processed using a double subtraction method described in the Supporting Information, Methods, and the processed spectra for each time delay were fit to sums of Fano line shapes using Igor Pro (a sample of the fits appears in Figure S2).

■ ASSOCIATED CONTENT

Supporting Information

The Supporting Information is available free of charge on the ACS Publications website at DOI: 10.1021/acs.jpclett.6b01453.

Detailed sample preparation, ultrafast SERS instrumentation (Figure S1), data collection, processing and fitting details (Figure S2 and S3), pump power dependence (Figure S4), Fano q parameter time dependence (Figure S5), and Fano q parameter power dependence (Figure S6) (PDF)

■ AUTHOR INFORMATION

Corresponding Author

*E-mail: rrf@umn.edu. Phone: 612.624.2501. Address: 207 Pleasant St SE, University of Minnesota, Minneapolis, MN 55455.

Notes

The authors declare no competing financial interest.

■ ACKNOWLEDGMENTS

This material is based on work supported by the Air Force Office of Scientific Research under AFOSR Award No. FA9550-15-1-0022. Parts of this work were carried out in the Characterization Facility, University of Minnesota, which receives partial support from the NSF through the MRSEC program. The authors thank Prof. David Jonas and Prof. Ara Apkarian for helpful discussions and the research group of Prof. David Blank for access to the UV−visible spectrophotometer used for sample characterization.

■ REFERENCES

(1) Brongersma, M. L.; Halas, N. J.; Nordlander, P. Plasmon-Induced Hot Carrier Science and Technology. *Nat. Nanotechnol.* **2015**, *10*, 25−34.

(2) Linic, S.; Aslam, U.; Boerigter, C.; Morabito, M. Photochemical Transformations on Plasmonic Metal Nanoparticles. *Nat. Mater.* **2015**, *14* (6), 567−576.

(3) Moskovits, M. The Case for Plasmon-Derived Hot Carrier Devices. *Nat. Nanotechnol.* **2015**, *10*, 6−8.

(4) Mukherjee, S.; Libisch, F.; Large, N.; Neumann, O.; Brown, L. V.; Cheng, J.; Lassiter, J. B.; Carter, E. A.; Nordlander, P.; Halas, N. J. Hot Electrons Do the Impossible: Plasmon-Induced Dissociation of H_2 on Au. *Nano Lett.* **2013**, *13* (1), 240−247.

(5) Mukherjee, S.; Zhou, L.; Goodman, A. M.; Large, N.; Ayala-Orozco, C.; Zhang, Y.; Nordlander, P.; Halas, N. J. Hot-Electron-Induced Dissociation of H_2 on Gold Nanoparticles Supported on SiO_2. *J. Am. Chem. Soc.* **2014**, *136* (1), 64−67.

(6) Hartland, G. V. Optical Studies of Dynamics in Noble Metal Nanostructures. *Chem. Rev.* **2011**, *111* (6), 3858−3887.

(7) Aruda, K. O.; Tagliazucchi, M.; Sweeney, C. M.; Hannah, D. C.; Weiss, E. A. The Role of Interfacial Charge Transfer-Type Interactions in the Decay of Plasmon Excitations in Metal Nanoparticles. *Phys. Chem. Chem. Phys.* **2013**, *15* (20), 7441−7449.

(8) Jarrett, J. W.; Zhao, T.; Johnson, J. S.; Knappenberger, K. L. Investigating Plasmonic Structure-Dependent Light Amplification and Electronic Dynamics Using Advances in Nonlinear Optical Microscopy. *J. Phys. Chem. C* **2015**, *119* (28), 15779−15800.

(9) Major, T. A.; Lo, S. S.; Yu, K.; Hartland, G. V. Time-Resolved Studies of the Acoustic Vibrational Modes of Metal and Semiconductor Nano-Objects. *J. Phys. Chem. Lett.* **2014**, *5* (5), 866−874.

(10) Crut, A.; Maioli, P.; Del Fatti, N.; Vallée, F. Optical Absorption and Scattering Spectroscopies of Single Nano-Objects. *Chem. Soc. Rev.* **2014**, *43* (11), 3921−3956.

(11) Boerigter, C.; Campana, R.; Morabito, M.; Linic, S. Evidence and Implications of Direct Charge Excitation as the Dominant Mechanism in Plasmon-Mediated Photocatalysis. *Nat. Commun.* **2016**, *7*, 10545.

(12) Hwang, Y. N.; Jeong, D. H.; Shin, H. J.; Kim, D.; Jeoung, S. C.; Han, S. H.; Lee, J. S.; Cho, G. Femtosecond Emission Studies on Gold Nanoparticles. *J. Phys. Chem. B* **2002**, *106* (31), 7581−7584.

(13) Beversluis, M. R.; Bouhelier, A.; Novotny, L. Continuum Generation from Single Gold Nanostructures through Near-Field Mediated Intraband Transitions. *Phys. Rev. B: Condens. Matter Mater. Phys.* **2003**, *68* (11), 115433.

(14) Heritage, J. P.; Bergman, J. G.; Pinczuk, A.; Worlock, J. M. Surface Picosecond Raman Gain Spectroscopy of a Cyanide Monolayer on Silver. *Chem. Phys. Lett.* **1979**, *67* (2), 229−232.

(15) Kozich, V.; Werncke, W. The Vibrational Pumping Mechanism in Surface-Enhanced Raman Scattering: A Subpicosecond Time-Resolved Study. *J. Phys. Chem. C* **2010**, *114* (23), 10484−10488.

(16) van Schrojenstein Lantman, E. M.; Deckert-Gaudig, T.; Mank, A. J. G.; Deckert, V.; Weckhuysen, B. M. Catalytic Processes Monitored at the Nanoscale with Tip-Enhanced Raman Spectroscopy. *Nat. Nanotechnol.* **2012**, *7* (9), 583−586.

(17) Sun, M.; Xu, H. A Novel Application of Plasmonics: Plasmon-Driven Surface-Catalyzed Reactions. *Small* **2012**, *8* (18), 2777−2786.

(18) Kang, L.; Xu, P.; Zhang, B.; Tsai, H.; Han, X.; Wang, H. L. Laser Wavelength- and Power-Dependent Plasmon-Driven Chemical Reactions Monitored Using Single Particle Surface Enhanced Raman Spectroscopy. *Chem. Commun.* **2013**, *49* (33), 3389−3391.

(19) Choi, H.-K.; Park, W.-H.; Park, C.-G.; Shin, H.-H.; Lee, K. S.; Kim, Z. H. Metal-Catalyzed Chemical Reaction of Single-Molecules Directly Probed by Vibrational Spectroscopy. *J. Am. Chem. Soc.* **2016**, *138* (13), 4673−4684.

(20) Stiles, P. L.; Dieringer, J. A.; Shah, N. C.; Van Duyne, R. P. Surface-Enhanced Raman Spectroscopy. *Annu. Rev. Anal. Chem.* **2008**, *1*, 601−626.

(21) Fang, Y.; Seong, N.-H.; Dlott, D. D. Measurement of the Distribution of Site Enhancements in Surface-Enhanced Raman Scattering. *Science* **2008**, *321* (5887), 388−393.

(22) Kleinman, S. L.; Ringe, E.; Valley, N.; Wustholz, K. L.; Phillips, E.; Scheidt, K. A.; Schatz, G. C.; Van Duyne, R. P. Single-Molecule Surface-Enhanced Raman Spectroscopy of Crystal Violet Isotopologues: Theory and Experiment. *J. Am. Chem. Soc.* **2011**, *133* (11), 4115−4122.

(23) Darby, B. L.; Etchegoin, P. G.; Le Ru, E. C. Single-Molecule Surface-Enhanced Raman Spectroscopy with Nanowatt Excitation. *Phys. Chem. Chem. Phys.* **2014**, *16* (43), 23895−23899.

(24) Hao, E.; Schatz, G. C. Electromagnetic Fields around Silver Nanoparticles and Dimers. *J. Chem. Phys.* **2004**, *120* (1), 357−366.

(25) Kleinman, S. L.; Frontiera, R. R.; Henry, A.-I.; Dieringer, J. A.; Van Duyne, R. P. Creating, Characterizing, and Controlling Chemistry with SERS Hot Spots. *Phys. Chem. Chem. Phys.* **2013**, *15* (1), 21−36.

(26) Skadtchenko, B. O.; Aroca, R. Surface-Enhanced Raman Scattering of P-Nitrothiophenol. *Spectrochim. Acta, Part A* **2001**, *57* (5), 1009−1016.

(27) Kim, K.; Shin, D.; Kim, K. L.; Shin, K. S. Surface-Enhanced Raman Scattering of 4,4′-dimercaptoazobenzene Trapped in Au Nanogaps. *Phys. Chem. Chem. Phys.* **2012**, *14* (12), 4095−4100.

(28) Berg, C. M.; Sun, Y.; Dlott, D. D. Temperature-Dependent Dynamic Response to Flash Heating of Molecular Monolayers on Metal Surfaces: Vibrational Energy Exchange. *J. Phys. Chem. B* **2014**, *118* (28), 7770−7776.

(29) Frontiera, R. R.; Henry, A. I.; Gruenke, N. L.; Van Duyne, R. P. Surface-Enhanced Femtosecond Stimulated Raman Spectroscopy. *J. Phys. Chem. Lett.* **2011**, *2* (10), 1199−1203.

(30) Frontiera, R. R.; Gruenke, N. L.; Van Duyne, R. P. Fano-like Resonances Arising from Long-Lived Molecule-Plasmon Interactions in Colloidal Nanoantennas. *Nano Lett.* **2012**, *12* (11), 5989−5994.
(31) Dey, S.; Banik, M.; Hulkko, E.; Rodriguez, K.; Apkarian, V. A.; Galperin, M.; Nitzan, A. Observation and Analysis of Fano-like Lineshapes in the Raman Spectra of Molecules Adsorbed at Metal Interfaces. *Phys. Rev. B: Condens. Matter Mater. Phys.* **2016**, *93* (3), 035411.
(32) Del Fatti, N.; Vallée, F.; Flytzanis, C.; Hamanaka, Y.; Nakamura, A. Electron Dynamics and Surface Plasmon Resonance Nonlinearities in Metal Nanoparticles. *Chem. Phys.* **2000**, *251* (1−3), 215−226.
(33) Lässer, R.; Smith, N. V.; Benbow, R. L. Empirical Band Calculations of the Optical Properties of D-Band Metals. I. Cu, Ag, and Au. *Phys. Rev. B: Condens. Matter Mater. Phys.* **1981**, *24* (4), 1895−1909.
(34) Haug, T.; Klemm, P.; Bange, S.; Lupton, J. M. Hot-Electron Intraband Luminescence from Single Hot Spots in Noble-Metal Nanoparticle Films. *Phys. Rev. Lett.* **2015**, *115* (6), 067403.
(35) Boerigter, C.; Aslam, U.; Linic, S. Mechanism of Charge Transfer from Plasmonic Nanostructures to Chemically Attached Materials. *ACS Nano* **2016**, *10* (6), 6108−6115.
(36) Hugall, J. T.; Baumberg, J. J. Demonstrating Photoluminescence from Au Is Electronic Inelastic Light Scattering of a Plasmonic Metal: The Origin of SERS Backgrounds. *Nano Lett.* **2015**, *15* (4), 2600−2604.
(37) Stranahan, S. M.; Willets, K. A. Super-Resolution Optical Imaging of Single-Molecule SERS Hot Spots. *Nano Lett.* **2010**, *10* (9), 3777−3784.
(38) Lee, P. C.; Meisel, D. Adsorption and Surface-Enhanced Raman of Dyes on Silver and Gold Sols. *J. Phys. Chem.* **1982**, *86* (17), 3391−3395.
(39) Shim, S.; Mathies, R. A. Generation of Narrow-Bandwidth Picosecond Visible Pulses from Broadband Femtosecond Pulses for Femtosecond Stimulated Raman. *Appl. Phys. Lett.* **2006**, *89* (12), 121124.

DOI: 10.1021/acs.jpclett.6b01453
J. Phys. Chem. Lett. 2016, 7, 3179−3185